Advanced International Journal for Research (AIJFR)
E-ISSN: 3048-7641 ● Website: www.aijfr.com ● Email: editor@aijfr.com

Analysis of Aerodynamic Characteristics for a Missile Geometry in the Supersonic and Hypersonic Flow Regimes

M Ananth Padmanabha[1], Bhoomika Prasad[2], Jayahar Sivasubramanian[3]

[1,2,3] Department of Aerospace and Automotive Engineering, M. S. Ramaiah University of Applied Sciences, Bangalore, India

Abstract

The aim of this paper is to present an aerodynamic analysis of the N1G missile geometry at supersonic and hypersonic Mach numbers to understand how the behaviour varies as it transits from the supersonic to the hypersonic flow regime. The study contemplates to provide new insights into the missile aerodynamic performance which includes lift and drag coefficients using computational fluid dynamics (CFD). The first part of the study involves the validation of the results from the computational simulations with the experimental data available from the wind tunnel tests [3]. This validation establishes the accuracy and robustness of the numerical method. The research further extends to analyse the aerodynamic performance in the supersonic and hypersonic regime, for the same missile geometry. The paper intends to feature the differences in the aerodynamics of the missile as it goes beyond the supersonic threshold. Variations in the flow pattern, shock wave and aerodynamic forces (lift and drag) were observed and discussed. This work will impart a valuable analysis of the complex flow phenomena which is associated with the hypersonic regime, providing necessary data for the optimisation of the geometry. The study also lays the groundwork for better computational models, which are essential for developments in missile technology and other aerospace applications that operate in the hypersonic regime.

Keywords: CFD, Missile, Aerodynamic Characteristics, Shock Wave, Supersonic Flow, Hypersonic Flight.

1. Introduction

Missiles are advanced guided projectiles designed for both civilian and military applications. These are self-propelled and guided weapons proficient in delivering payloads with high precision and accuracy to specified targets. Aerodynamics is said to be the study of the behaviour of airflow around the body in order to predict and understand the aerodynamic characteristics such as lift coefficient (C_L) and drag coefficient (C_D). Aerodynamics plays a crucial role in the design and development of the missile. Moreover, the efficiency of the missile and its accuracy in hitting the target is also influenced by its aerodynamic performance. Our study involves the analysis of the aerodynamic performance of the N1G missile geometry, whose details have been taken from [2]. The study includes the analysis of the lift and drag coefficients (C_L and C_D) for Mach 4 and 6, where in the analysis is performed for various angles of attack ranging from 0° to 6°. The analysis is done using the commercial software Ansys. First, the

validation for Mach 4 case has been done by comparing the results from the CFD simulation with the wind tunnel data from [3]. A grid convergence study has been carried out for 4° AoA at Mach 4. Then validation for Mach 4 case has been done by comparing the results from the numerical Simulation with the experimental data obtained from [3]. A comparative study is performed to check the difference in the performance as the missile transits from supersonic to hypersonic speed. As seen in previous research, the researchers have performed the aerodynamic analysis up to Mach 4 and there was a lack of essential flow parameters and analysis in Hypersonic. This motivated us to study and analyse the aerodynamic characteristics of the missile in the Supersonic and Hypersonic flow regimes. This study will provide an understanding of the change in flow physics from Supersonic to hypersonic, this data can be used for the optimisation process in order to improve the stability and aerodynamic coefficients which in turn will improve the overall performance and range of the missile, which will be our future work.

2. Literature Review and Objective

A. Jameson et al. [1] – The significance of computational fluid dynamics in aeroplane design was discussed in this paper. They concentrated on the aerodynamic design problem and examined how this process has advanced. The computational expenses of this present method are compared to those associated with different aerodynamic optimization techniques. Two case examples have been provided for demonstrating the advantages of using automated aerodynamic optimization. The first instance demonstrates the use of such software across an entire aircraft-design endeavours, while the second case demonstrates how much the aerodynamic design cycle may be shortened. Nenad Vidanovic et al. [3] - The objective of this work aimed to come up with an effective fin design employing numerical optimization techniques while considering fluid and structural interactions into account. The computational technique was used to investigate the fluid structural interactions over a tightly linked area. This was done with high levels of accuracy and reliability. This paper contains the necessary dimensions and flow parameters for the missile. Also, the experimental data from the wind tunnel [15] have been shortlisted. Amandeep Singh [4] - The aerodynamic characteristics of an anti-aircraft missile are computed using Ansys solver. Computation extends from subsonic to supersonic Mach at standard sea level conditions. this gives an idea of how the Drag and moment vary with Mach number. Sebastian Marian Zaharia et al. [5] - The CFD simulation conducted in this paper was carried out on a missile with a ballistic missile geometry with a new construction to determine the flight characteristics and aerodynamic configuration. In order to precisely determine the points on the geometry where the stress and strain were greatest during the structural analysis procedure, the finite element method was used. It has been inferred from the literature review that there is a need to explore the hypersonic regime and understand how the flow changes across the missile as we transit to Mach 6. The objective of the paper is to compare the flow features of the missile body for Mach 4 and Mach 6 at different angle of attacks ranging from 0° to 6°. Results of Mach 4 will be validated against the experimental data, and Mach 6 will have grid convergence.

3. Simulation Setup and Numerical Methods

A. Geometry creation:

For our study N1G model was opted, the missile model was selected from [2]. The missiles 3-D model was created in Catia V5 using the dimensions available in the literature [2] as shown in Figure 2. The model was then imported in Ansys design modular (DM) and a computational fluid domain of length 4200

mm, breadth 3000 mm and height 3000 mm was created as shown in Figure 3. The analysis involves Mach 4 and 6, whose influence will be closer to the missile body and will be more like a uniform streamline away from the body. Thus, the domain is made small and mesh is made finer close to the body, this reduces the computational time.

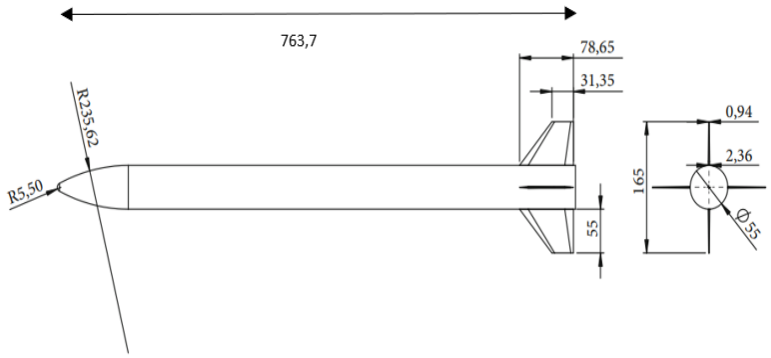

Figure 1: Missile Geometry Dimensions in mm.

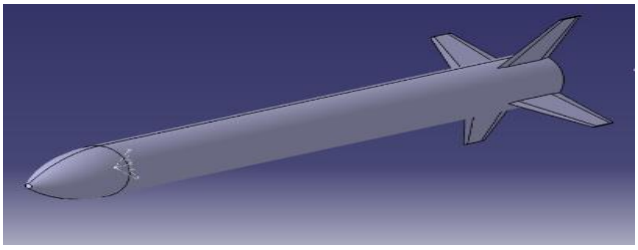

Figure 2: 3D missile model in Catia-V5.

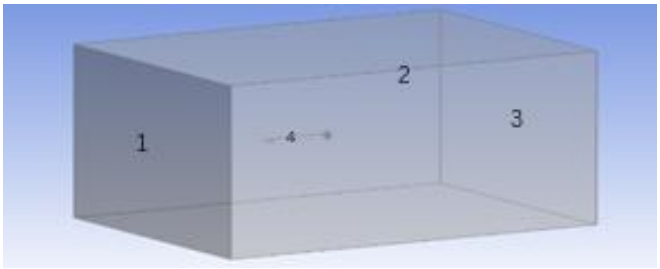

1 (inlet) – Pressure Far Field
2 (Domain walls) – Pressure Far Field
3 (Outlet) – Pressure outlet
4 (Missile body) – Adiabatic wall

Figure 3: 3D Domain with Boundary condition.

B. Mesh Generation:

The geometry has been discretized by mesh module into a 3D unstructured tetrahedral mesh as shown in figure 4. A 3D mesh allows for a detailed representation of the geometry and structure in the 3D space. The use of boundary layers makes the mesh finer near the missile body which increases exponentially when moving away from the body, which is seen in Figure 5.

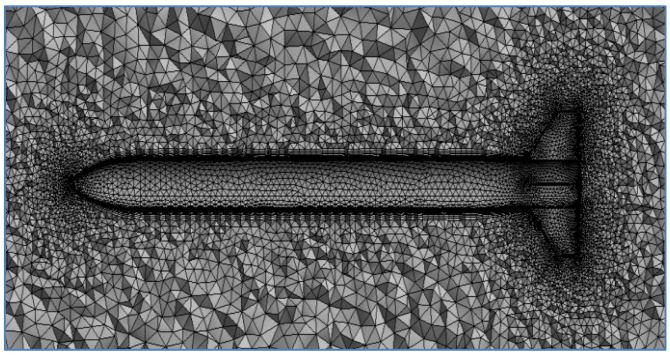

Figure 4: 3D unstructured mesh.

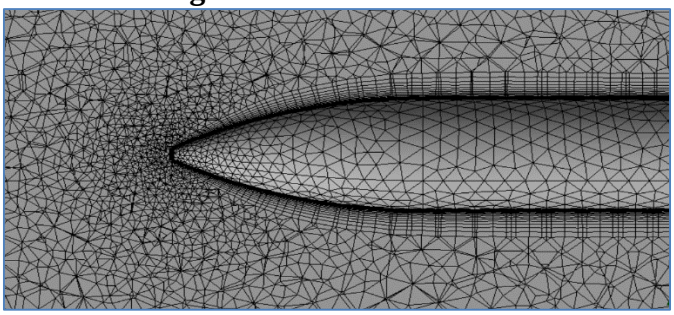

Figure 5: Mesh with inflation layers.

C. Numerical Methods:

Ansys Fluent flow solver which is based on finite volume method where the conservation equations are solved, is used in this study. To model and simplify the control volume, Navier-Strokes equations are used. The convergence criteria were set to 10^{-5}. Referring to [3] Density-based steady state type solver with Implicit formulation (coupled scheme), AUSM flux type [8] was selected for the solution method. Ideal gas is considered with Sutherland viscosity model. The gradient was selected to be least square cell-based, where in the order for pressure, the upwind scheme for density, momentum, turbulent kinetic energy, specific dissipation rate and energy for spatial discretization was taken to be second order. SST k – ω [9,10] turbulent model was selected as it is efficient in solving complex flow field at high speed. Flow residuals and aerodynamic coefficient changes were monitored to assess the convergence during the simulation. Courant number, which is the main control over time-stepping scheme is varied from 0.1 to 1. The free stream conditions such as static pressure and temperature are given in Table 1. These conditions are calculated from the Mach number and altitude graph [3] for Mach 4 and for Mach 6, free stream conditions are taken from [13] as there are no sufficient parameters available. [13] has the wind tunnel parameters at Mach 6 hence it is considered.

Table 1: Free stream conditions

Inlet Parameters	Mach 4	Mach 6
Static Pressure (Pa)	8786.68	660.591
Static Temperature (K)	218.16	52.439

4. Results and Discussion

For validation we have performed the grid convergence study for AoA of 4.03° at Mach 4 as shown in Figure 6. The CFD results of aerodynamic coefficients (C_L and C_D) for AoA 4.03° and 6.08° at Mach 4 have been compared with the experimental result obtained from the wind tunnel testing [[3],[11],[12]] shown in Table 2.

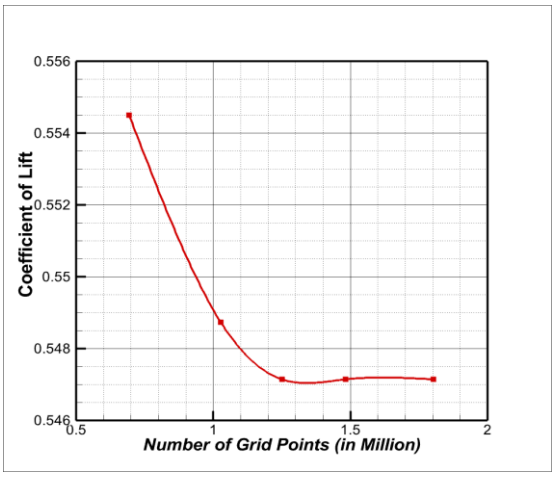

Figure 6: Grid convergence study

From Figure 6 we see how the C_L varies for coarse, medium and fine grids. As the value of C_L is the same for 1200000, 1400000 and 1800000 grid points, we select 1200000 mesh for our further analysis in order to reduce the computational time.

Table 2: Comparison of simulation results and experimental data [3] for Mach 4

α	C_L (exp)	C_L (Fluent)	Error (%)	C_D (exp)	C_D (Fluent)	Error (%)
4.03	0.532	0.547	2.819	0.3931	0.4025	2.391
6.08	0.881	0.903	2.497	0.4539	0.4627	1.938

The validation of the numerical results with experimental data [3] have been compared in Table 2. For the assumed Flow parameters (Table 1) the error is considerably low, when compared to the numerical solution in [3], this is possible due to the difference in the flow parameters.

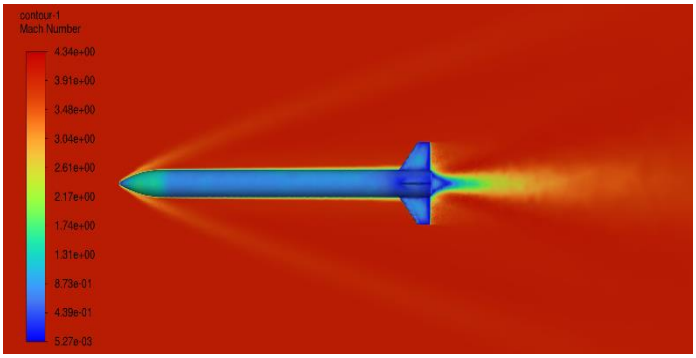

Figure 7: Mach contour for α=0° at Mach 4.

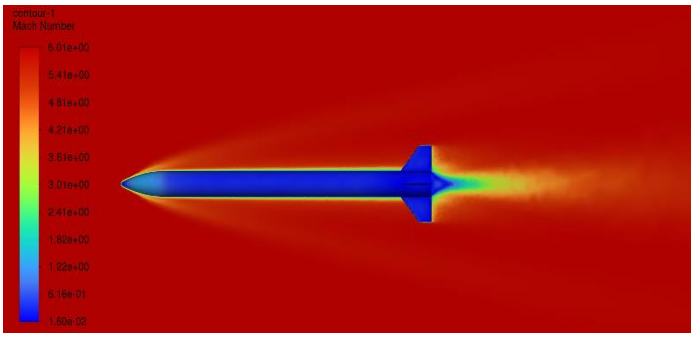

Figure 8: Mach contour for α=0° at Mach 6.

From Figure 7 and Figure 8 we can infer that at the AoA 0° the flow is symmetric on the upper and lower surface of the missile. As the Mach number increases the shock wave intensifies. The shock wave at the nose in Figure 7 is smooth and less intense, pressure build-up is moderate. In Figure 8, at the nose there is a bow shock formed. As the flow transits from Mach 4 to 6 the shock wave becomes more prominent and would cover a larger portion of the body. Around the fin the shock is smooth and moderate for Mach 4 whereas for Mach 6 the airflow around the missile becomes highly turbulent and separated due to stronger shock formed. The wake region is smaller for Mach4 compared to Mach 6 as the flow is less chaotic in Mach 4. From Figure 9 and Figure 10 we see that at higher AoA 6, the flow is asymmetric over the missile. At Mach 6 the flow becomes more complex. The shock formed is stronger and the shock angle decreases. The presence of shock wave causes an abrupt increase in temperature and pressure across the shock.

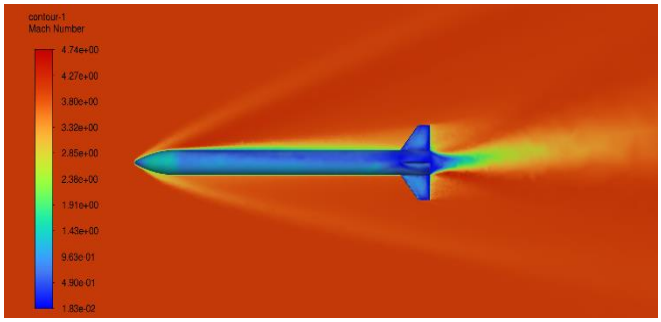

Figure 9: Mach contour for α=6° at Mach 4.

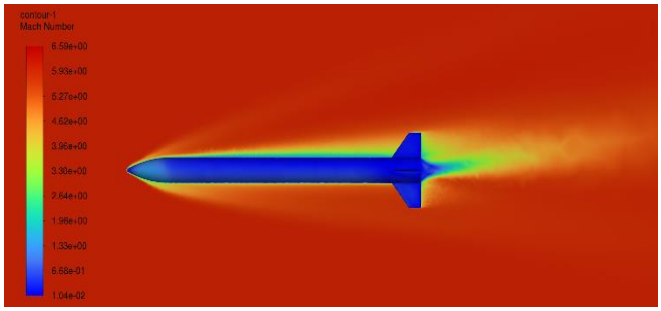

Figure 10: Mach contour for α=6° at Mach 6.

The flow downstream of the shock is characterized by high pressure and low velocity compared to the free stream condition. The pressure and temperature increase are seen higher in Mach 6 leading to higher pressure gradient and drag. At AoA 6, at Mach 6 the wake is more dynamic and turbulent where it is more stable in Mach 4. The stronger shock formed at Mach 6 with a series of expansion fans, which results in more significant flow separation from the missile surface. Due to the presence of recirculation between

the shock and boundary layer leads to vortices in the wake region, which contributes to increased drag affecting the overall aerodynamic performance of the missile. Comparing the Figure 9 and Figure 10 with Figure 7 and Figure 8, it is observed that the presence of a flow separation is due to an increase in pressure gradient on the surface. At Mach 6, the flow separation becomes more noticeable than at Mach 4, hence increasing the drag. From AoA 0° to 6°, the same trend is seen.

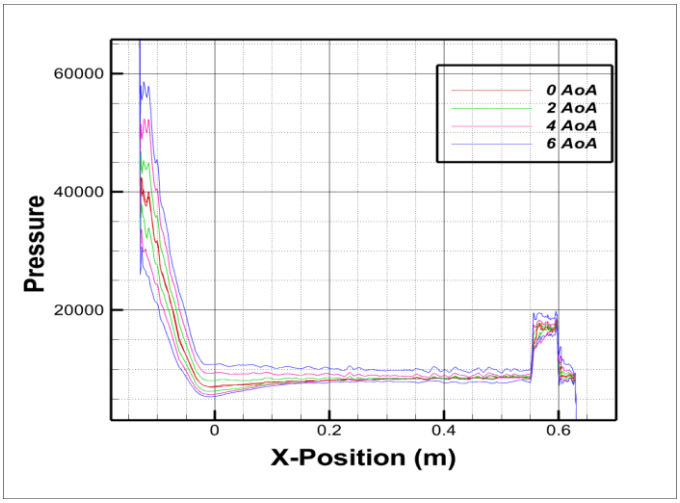

Figure 11: Plot of pressure distribution on the missile body for Mach 4 and different AoA.

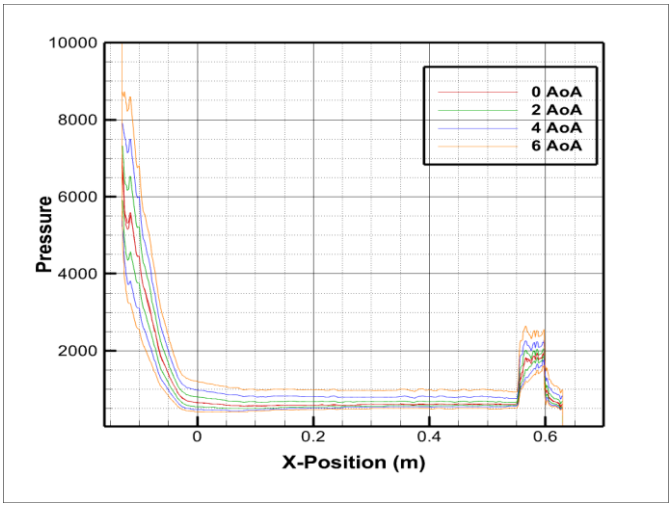

Figure 12: Plot of pressure distribution on the missile body for Mach 6 and different AoA.

From Figure 11, Figure 12 we can observe that as the missile encounters the free stream there is formation of bow shock as shown in the Mach contours from Figure 7 to Figure 10, due to which across the bow shock at the nose there is an increase in pressure. As the flow moves along the body the pressure will decrease and become uniform. As the flow moves further and it impinges on the windward side of the fin, the flow experiences compression which in turn leads to a localized increase in pressure. This pressure increase is due the flow being deflected which undergoes compression due to its curvature. There is a decrease in pressure on the leeward side of the fin, as there is flow separation, and is the result of separated boundary layer and the low-pressure wake behind the fin.

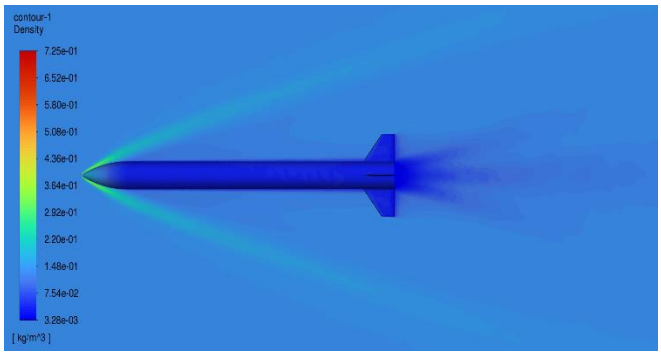

Figure 13: Density contour for α=0° at Mach 4.

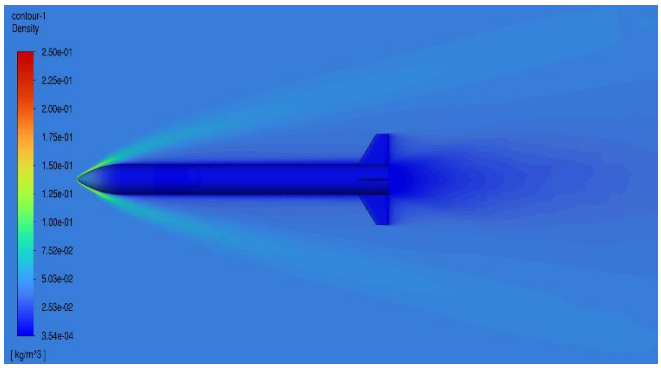

Figure 14: Density contour for α=0° at Mach 6.

In Figure 13 and Figure 14 we observe that at 0° AoA There is a uniform density distribution over the missile with the highest density at the nose. As the Mach increase from 4 to 6 the shock wave becomes more concentrated and also the shock angle decreases. At Mach 4 the wake region behind the missile exhibits a unique behaviour where it splits and conforms to the shape of the fins, whereas it is not seen in Mach 6.

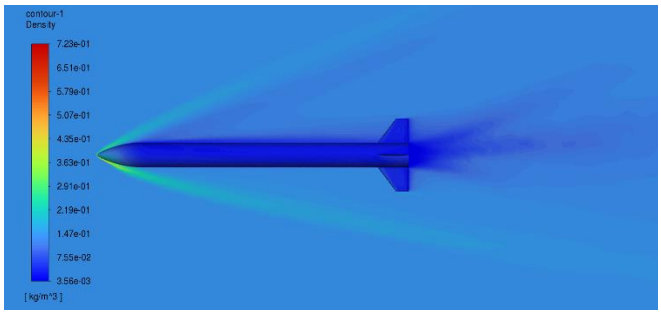

Figure 15: Density contour for α=6° at Mach 4.

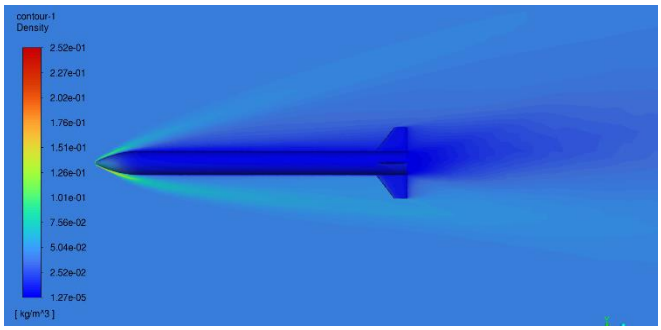

Figure 16: Density contour for α=6° at Mach 6.

In Figure 15 and Figure 16 we see an asymmetric distribution with increase in AoA, there is a higher density on the lower surface of the nose compared to the upper surface. The increase in AoA also influences the wake region.

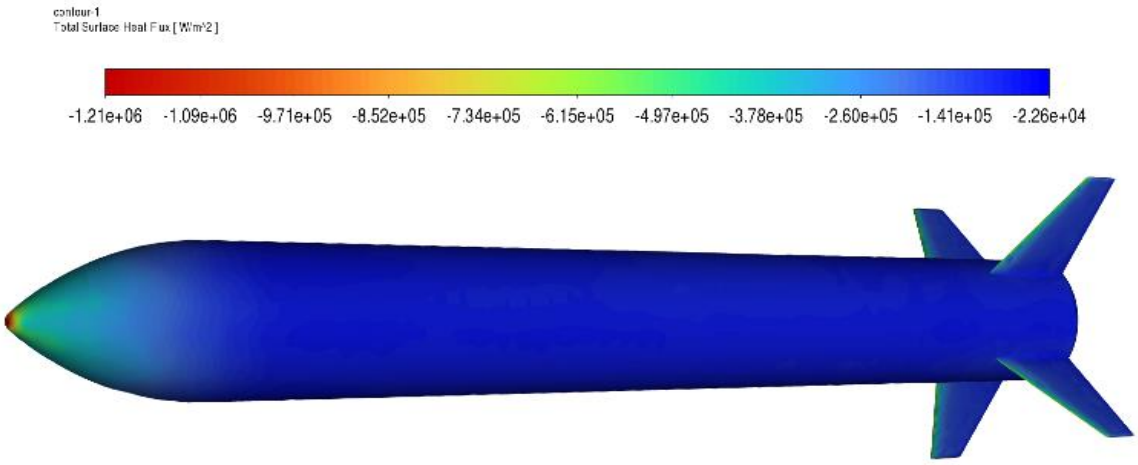

Figure 17: Total surface heat flux for Mach 4 at α=0°

Figure 17 and Figure 18 shows the total heat flux on the surface of the missile. The surface temperature reaches as high as 1300K. As in Ansys the heat flux is shown in negative values, one of the reasons is that the temperature on the missile is higher compared to the domain, so the negative sign shows that there is heat transfer from missile into the domain. Hence the contour with the red coloured region is highest and blue coloured region is the lowest heat flux over the missile body surface.

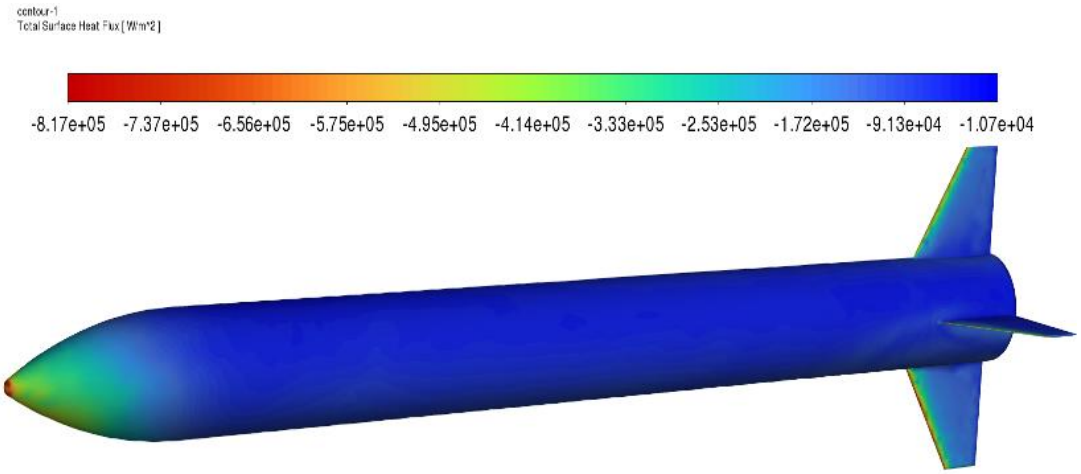

Figure 18: Total surface heat flux for Mach 4 at α=6°

In Figure 17 and Figure 18 we observe the highest heat flux at the tip of the nose (which is the stagnation point), and we can visualize the linear decrease in heat flux from the nose tip to the missile body. The windward side of the fin also experiences maximum heat flux as there is shock-shock interaction and shock impingement, this region has a greater pressure than the leeward side as seen in Figure 11 and Figure 12. For a given Mach number as the angle of attack increases from α=0° to α=6° the surface heat flux distribution becomes asymmetric and there is more heat flux on the lower surface of the nose which is due to the shock wave being closer (observed in the Mach and density contours). As the Mach number increases the total surface heat flux will increase due to stronger bow shock and relative decrease in shock angle.

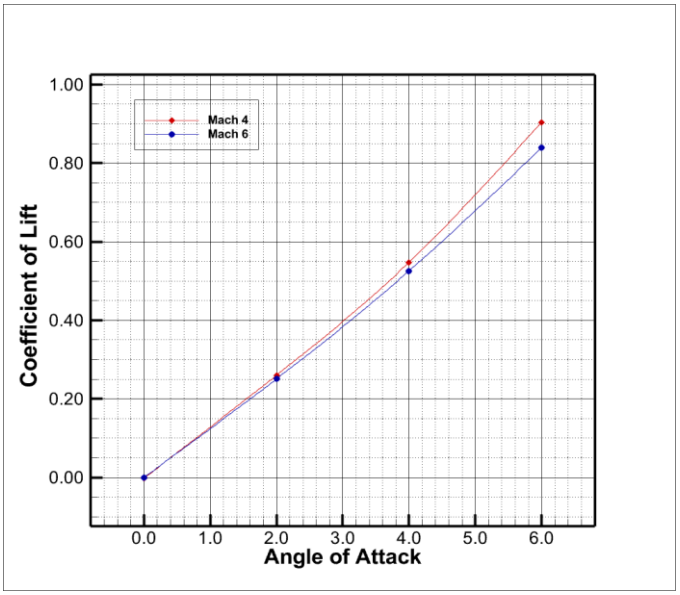

Figure 19: Plot of C_L vs AoA for Mach 4 and Mach 6

From figure 19 it is observed that, as the AoA increases the C_L (lift coefficient) increases for both Mach 4 and Mach 6. Initially at AoA 0° the pressure on the upper and lower surface is almost the same, but as the AOA increases the pressure difference also increases. The pressure on the upper surface is low

compared to the pressure on the lower surface at higher AoA, leading to increased C_L. At higher AoA the curvature of the nose contributes to higher C_L as the flow is deflected downwards. In figure 19 it is seen that the values of C_L are larger for Mach 4 compared to Mach 6.

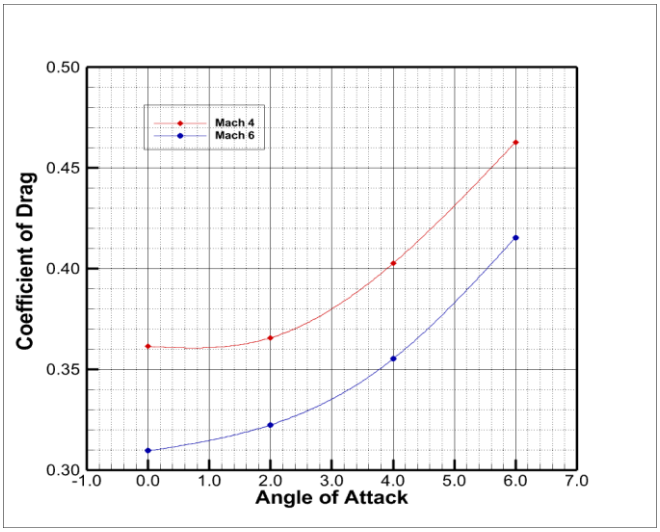

Figure 20: Plot of Cd vs AoA for Mach 4 and Mach 6.

From Figure 20 we can infer that C_D increases with AoA and is larger for Mach 4. The stronger shock wave formed at Mach 6 compared to Mach 4 increases more as AoA increases. This contributes to the increase in wave drag, as explained in the Mach contour earlier. At higher AoA the pressure difference in increased leading to increased pressure drag. The increase in the separation bubble also contributes to increasing the drag.

5. Conclusions

In our study we have performed the aerodynamic analysis of the missile at supersonic and hypersonic speed (Mach 4 and Mach 6), this analysis also involves AoA varying from 0° to 6°. In order to choose the suitable grid, a grid convergence study was performed where 1200000 grid points were found suitable for the study. The aerodynamic characteristics C_L and C_D obtained from simulation for 4.03° and 6.08° have been compared with the experimental data from wind tunnel testing [3, 15].

The difference in C_L for 4.03° and 6.08° were 2.74% and 2.43% respectively, whereas C_D was 2.391% and 1,938% respectively. The error percentage has been decreased significantly which is almost 1.5% when compared to the reference paper [3]. From the Analysis we conclude that as the angle of attack increases the lift and drag coefficient increases for a Mach number. The Lift and drag coefficient values are high for Mach 4 compared to Mach 6. This is due to various factors which include the velocity of the missile, temperature affecting the missile surface, the altitude at which the missile is flying and etc, missile will exhibit various aerodynamic challenges with aerodynamic heating and instability due to increased airflow and compressibility. The specific aerodynamic characteristics, including lift-to-drag ratio, pressure distribution and shock wave patterns play a vital role in describing the overall efficiency and accuracy while in flight. At Mach 6, the missile undergoes more significant challenges, the aerodynamic characteristic here indicates the higher drag and potential control issues at this speed. To improve the effectiveness of the missile's performance, several optimization measures and processes can be

implemented. Streamlining the aerodynamic design and minimizing the protrusions can improve the overall efficiency by increasing in lift and by reducing the drag. Optimization efforts are crucial to address these concerns, and further analysis is needed to optimize the design in order to improve the missile's efficiency, performance and manoeuvrability. This paper gives an overall understanding of the changes in aerodynamic performance at hypersonic Mach number, this can be taken reference to optimise the geometry in order to get better stability, lift-to-drag ratio. This intern improves the range of the missile, which will be the future scope of our study.

References

1. A. Jameson and J. C. Vassberg, (2001), "*Computational fluid dynamics for aerodynamics design: its current and future impact*." 39th AIAA Aerospace Sciences Meeting & Exhibit, 2001.
2. Ahmet Şumnu, İbrahim Halil Güzelbey and Orkun Öğücü, (2020) "*Aerodynamic Shape Optimization of a Missile Using a Multiobjective Genetic Algorithm*", *International Journal of Aerospace Engineering*, 2020.
3. Nenad Vidanovic´, Boško Rašuo , Gordana Kastratovic´, Stevan Maksimovic´, Dušan Curci˘c´, Marija Samardžic´. (2017) "*Aerodynamic–structural missile fin optimization*." *Aerospace Science and Technology*, Volume 65, June 2017, Pages 26-45
4. Amandeep Singh, (2020) "*Aerodynamic Analysis on Missile Design*" *International Journal of Scientific Development and Research*, ISSN: 2455-2631 IJSDR2010034.
5. Sebastian Marian Zaharia, Rareș Ioan Stefaneanu, (2016) "*CFD simulation and FEA analysis of a Ballistic Missile*." *Journal of Industrial Design and Engineering Graphics*, Vol. 11, 2, 2016.
6. J.D. Anderson Jr., (1995) "*Computational Fluid Dynamics, the Basics with Applications*", McGraw-Hill, Inc., 1995.
7. Habip ASAN, Mehmet AKC, (1999) "*Prediction of Aerodynamic Characteristics of missile with circular and Noncircular cross sections*." *Tr. J. of Engineering and Environmental Science*, 1999.
8. M.S. Liou, (1996), "*A sequel to AUSM: AUSM+*", *J. Comput. Phys*. 129 (1996) 364–382.
9. F.R. Menter, (1992) "*Performance of popular turbulence models for attached and separated adverse pressure gradient flows*." *AIAA J*. 30 (8) (1992) 2066–2072.
10. Mohammad Javad Ameri, Mohammad Reza Heidari, Hashem Nowruzi, Amin Najafi, (2019) "*Analysis of Different Turbulence Models in Simulation of Hypersonic Flow in the Wind Tunnel*." *American Journal of Mechanical Engineering*. 2019, 7(4), 172-180
11. D. Damljanovic, ´ B. Rašuo, (2010) "*Testing of calibration models in order to certify the overall reliability of the trisonic blowdown wind tunnel of VTI*", FME Trans. 38 (4) (2010) 167–172.
12. D. Damljanovic, ´ J. Isakovic, ´ B. Rašuo, (2013) "T-38 wind-tunnel data quality assurance based on testing of a standard model", *J. Aircr*. 50 (4) (2013) 1141–1149.
13. Jayahar Sivasubramanian1 and Hermann F. Fasel, (2015) "*Direct numerical simulation of transition in a sharp cone boundary layer at Mach 6: fundamental breakdown*", *J. Fluid Mech*. (2015), vol. 768, pp. 175–218.